Electronic Research Archive

https://www.aimspress.com/journal/era

ERA, 34(4): 2112–2135.
DOI: 10.3934/era.2026095
Received: 28 December 2025
Revised: 14 February 2026
Accepted: 26 February 2026
Published: 09 March 2026

Research article

Exponential consensus for uncertain fractional-order multi-agent systems via T-S fuzzy impulsive control strategy

Cancan Zhang, Huaiqin Wu* and Lifei Wang

School of Science, Yanshan University, Qinhuangdao 066001, China

* **Correspondence:** Email: huaiqinwu@ysu.edu.cn.

Abstract: In this paper, a new type of fractional-order multi-agent systems (FOMASs) with parameter uncertainties and Takagi-Sugeno (T-S) membership functions is developed on a directed communication topology graph. Unlike existing results that either adopt fixed-gain impulsive control or deal with fractional-order consensus without simultaneously considering communication efficiency and parameter uncertainties, we propose a codesigned T-S fuzzy (TSF) impulsive control framework. By collecting instantaneous local information, leader-following and leaderless distributed TSF impulsive controllers are designed to realize the exponential consensus for the proposed FOMASs, where the impulsive gain is dynamically adjusted by the same set of fuzzy rules describing the system. In addition, some sufficient conditions with regard to the exponential consensus of FOMASs are addressed in terms of linear matrix inequalities (LMIs). Compared with the traditional impulsive controllers with the fixed gain, the designed TSF impulsive controller has faster convergence speed to achieve the exponential consensus of FOMASs with uncertainty, and it has lower energy consumption. We then present an application example in a single-link manipulator to validate the practical efficacy for the proposed theoretical findings.

Keywords: T-S fuzzy; fractional-order multi-agent systems; fuzzy impulsive control; uncertain parameters; exponential consensus

1. Introduction

Multi-agent systems (MASs), which are capable of handling complex tasks through collaboration among agents, have been applied widely in quadrotor formation flying [1, 2], autonomous driving in artificial intelligence [3], mobile sensor networks [4], and differential mobile robot cooperative control [5]. As a special class of MASs, complex dynamical networks have attracted considerable research interest due to their ability to model various natural and engineered systems, including power grids, communication networks, and biological systems. Among the most fundamental collective behaviors in complex networks, synchronization and consensus have been extensively studied [6–8]. In MASs, each agent operates autonomously to achieve collective objectives by interacting within a shared environment. As a vital dynamical behavior, the consensus of MASs has attracted considerable attention from scholars in diverse fields due to the practical applications in drone formations, robotic swarms, and so on.

Generally, the consensus of MASs is mainly classified into two categories: leader-following consensus [9–11] and leaderless consensus [12, 13], to address distinct tasks in the engineering. The leaderless mode is utilized to incite distributed cooperation among agents, and the leader-following mechanism is employed to create target tracking in MASs.

The aforementioned works described MASs using integer-order differential operators, which depend only on local system information. Obviously, MASs with integer-order are unable to accurately characterize intrinsic system properties such as memory effects and nonlinear disturbance accumulation. More recently, MASs with fractional-order have received extensive attention from researchers owing to its memory and hereditary nature. Various consensus problems have been addressed within this framework, including consensus of linear fractional-order multi-agent systems (FOMASs) via distributed feedback control [14, 15], the consensus tracking problems for nonlinear FOMASs [16, 17], leader-following and leaderless consensus under adaptive protocols [18, 19].

To model and approximate intricate nonlinear systems, the TSF system model has been developed in multiple fields, such as inverted pendulum systems [20], electric power steering systems [21], and flight control systems [22], where a series of fuzzy rules are introduced in system model. Recently, some significant findings on consensus of fuzzy MASs have been established. For example, in [23], the optimal output consensus was discussed for TS fuzzy MASs (TSFMASs) via adaptive distributed control. In [24], the delay-dependent consensus criteria was proposed for fractional-order TSFMASs. In [25], the impulsive consensus was investigated for nonlinear fuzzy MASs under DoS attacks. In [26], the output consensus was discussed for leader-following TSFMASs via a bumpless transfer control strategy. In [27], by applying the event-triggered control strategy, the consensus issue was addressed for fuzzy FOMASs with uncertain topology.

In real world, the parameter disturbances caused by various sources, such as environmental changes, manufacturing, and assembly errors, inevitably occurs in practical engineering applications [28–30]. It is meaningful for us to consider the consensus of MASs subject to parameter disturbances. Very recently, in [29], the consensus was explored for FOMASs with uncertain parameter disturbances under DoS attacks by applying the designed impulsive security controller. In [30], the consensus criteria were derived for leader-following descriptor FOMASs with uncertain parameters under output feedback control.

Impulsive controllers have been extensively utilized for consensus tracking in FOMASs due to their fast response and low cost [29, 31]. In the existing works, most impulsive controllers are designed by using a fixed gain. However, in practical application, impulsive controllers with fixed gains bring a great reduction of flexibility. To overcome this drawback, fuzzy impulsive controllers, which consist of TSF rules and impulsive controllers, have been developed to solve successfully some control problems [28, 32–35]. For fuzzy impulsive control, the dynamic adjustment mechanism with fuzzy rules and membership functions can be applied to increase robustness for nonlinear systems with uncertainties. Recently, many efforts have been devoted to stabilization and synchronization in TSF systems. For example, in [33], fast fixed-time impulsive bipartite synchronization was discussed for TSF complex networks with signed graphs under the designed fuzzy impulsive controller. In [34], the TSF impulsive control was applied to address the stabilization of nonlinear systems with a time delay. In [35], applying fuzzy hybrid control, multisynchronization was achieved for interconnected memristor-based impulsive neural networks. In [28], the event-triggered fuzzy impulsive controller was used to achieve stochastic finite-time stability for TSF systems with parameter uncertainties.

However, despite these advancements, achieving exponential consensus for FOMASs with parameter uncertainties through adjustable gain impulsive controllers remains an unsolved problem. The application of the T-S fuzzy method for both uncertain system modeling and impulsive controller design in fractional-order systems has not been fully explored, which constitutes the primary motivation of this study.

In this paper, a new FOMASs with parameter uncertainties and T-S membership functions is developed on a directed communication topology graph. For the proposed network systems, this paper performs a leader-following/leaderless exponential consensus analysis. Under the designed fuzzy impulsive control strategies, several sufficient conditions concerning the exponential consensus are established in terms of linear matrix inequalities (LMIs). The principal contributions are summarized as:

1) Different from existing works [24, 27], an improved TSF fractional model is developed. This model clearly considers the uncertainty factor, thereby making it able to describe complex nonlinear dynamics more accurately.

2) A novel TSF impulsive control strategy is developed in which the control gain is dynamically adjusted according to TSF rules. Compared with the traditional fixed gain impulsive method [25, 29, 31], this tunable mechanism improves the robustness against system uncertainties.

3) By means of fractional-order Lyapunov stability theory, this paper derives several sufficient criteria for FOMASs consensus under leader-following and leaderless conditions, respectively.

The structure of this paper is organized as follows: in Section 2, several essential definitions, lemmas, and system models are introduced. Section 3 presents the sufficient conditions for ensuring the leader-following/leaderless exponential consensus of FOMASs. An application example respective to the single-link manipulator is then presented to verify the analytical results in Section 4. Finally, the conclusion is presented in Section 5.

Notations: see Table 1.

2. Preliminaries and model description

2.1. Graph theory

The network topology is represented by a directed graph $\mathcal{G}(\mathcal{V}_{\mathcal{G}}, \mathcal{E}_{\mathcal{G}})$, where $\mathcal{V}_{\mathcal{G}} = \{v_1, v_2, \ldots, v_N\}$ is nodes set, and $\mathcal{E}_{\mathcal{G}} \subset \mathcal{V}_{\mathcal{G}} \times \mathcal{V}_{\mathcal{G}}$ denotes edges set. $\mathcal{A} = [a_{ij}] \in R^{N\times N}$ is the adjacency matrix of graph $\mathcal{G}(\mathcal{V}_{\mathcal{G}}, \mathcal{E}_{\mathcal{G}})$. Let $a_{ij} \geq 0$ denote the weight of edge (v_i, v_j) with $a_{ij} > 0$ if $(v_i, v_j) \in \mathcal{E}_{\mathcal{G}}$ and $a_{ij} = 0$ otherwise. Assume that the directed graph contains no self-loops. The neighbor set of agent i in graph $\mathcal{G}$ is defined as $N_i = \{j, (v_i, v_j) \in \mathcal{E}_{\mathcal{G}}\}$. The matrix $\mathcal{L} = [l_{ij}] \in R^{N\times N}$ is the Laplace matrix, where $l_{ij} = -a_{ij}$ if $i \neq j$, and $l_{ii} = \sum_{j=1, j\neq i}^{N} a_{ij}$. Consider a root vertex v_0 with associated connection weights b_i. The diagonal connectivity matrix $\mathcal{B} = \mathrm{diag}\{b_1, b_2, \ldots, b_N\}$ satisfies $b_i > 0$ if leader v_0 is connected to follower v_i; otherwise, $b_i = 0$.

Table 1. Notations

Symbol	Represents
N^+	Positive integers set
R/R^+	Real / non-negative real numbers set
R^n	The set of n-dimensional vectors
$R^{N\times N}$	$N \times N$-dimensional matrices
I	Identify matrix
$P > 0$	P is a positive definite matrix
$\lambda_{min}(P)$	The smallest eigenvalue of P
C^n	The class of functions that are n-times continuously differentiable
$\Gamma(\cdot)$	Gamma function
$\|x\|_2$	$x \in R^n$, $\|x\|_2 = (\sum_{i=1}^n x_i^2)^{\frac{1}{2}}$
$\otimes$	Kronecker product of matrices
$\delta(\cdot)$	Dirac delta function

2.2. Preliminaries

Definition 1. *[36] For $t > t_0$, the Caputo fractional-order derivative of function $x(t) \in C^n([t_0, +\infty), R)$ is represented by*

$$ {}_{t_0}^{C}\mathcal{D}_t^{\alpha} x(t) = \frac{1}{\Gamma(n-\alpha)} \int_{t_0}^{t} \frac{x^{(n)}(s)}{(t-s)^{1-n+\alpha}} ds, $$

where $0 \le n-1 < \alpha \le n$, $\Gamma(m) = \int_0^\infty t^{m-1}e^{-t}dt$. For $\alpha \in (0,1]$, the preceding expression simplifies to

$$ {}_{t_0}^{C}\mathcal{D}_t^{\alpha} x(t) = \frac{1}{\Gamma(1-\alpha)} \int_{t_0}^{t} \frac{x'(s)}{(t-s)^{\alpha}} ds. $$

For computational convenience, the Caputo operator ${}_{t_0}^{C}\mathcal{D}_t^{\alpha}$ will be uniformly denoted as $\mathcal{D}^\alpha$ hereafter.

Definition 2. *[37] The general Mittag-Leffler (M-L) function $E_{a,b}(z)$ with parameters a, b is defined by*

$$ E_{a,b}(z) = \sum_{k=0}^{\infty} \frac{z^k}{\Gamma(ak+b)}. $$

For $b = 1$, it degenerates to the single-parameter case $E_a(z)$. When $a = b = 1$, it simplifies to an exponential function.

Definition 3. *[38] Let $\{t_k\}(k \in N^+)$ be an impulsive sequence. The average impulsive time interval T_a is defined such that for constants $\mathbb{N}_0 \ge 0$ and $T_a \in R^+$, the following inequality holds:*

$$ \frac{t-s}{T_a} - \mathbb{N}_0 \le \mathbb{N}(t,s) \le \frac{t-s}{T_a} + \mathbb{N}_0, $$

where $\mathbb{N}(t,s)$ represents the quantity of impulsive occurrences within the interval (s,t).

Lemma 1. *[36] Let $x(t) \in C^1(R, R^n)$. Then, for $\alpha \in (0, 1]$ and $t \geq t_0$, the subsequent inequality relationship holds:*

$$\mathcal{D}^\alpha x^\top(t) \mathrm{P} x(t) \leq 2x^\top(t) \mathrm{P} \mathcal{D}^\alpha x(t),$$

where $\mathrm{P} > 0$.

Lemma 2. *[36] For real vectors* x *and* y *that satisfy* $\mathrm{x}, \mathrm{y} \in R^n$*, arbitrary scalar* $\varepsilon > 0$*, and matrix* $\mathrm{Q} > 0$*, the subsequent matrix inequality is satisfied:*

$$2\mathrm{x}^\top \mathrm{y} \leq \varepsilon \mathrm{x}^\top \mathrm{Q} \mathrm{x} + \varepsilon^{-1} \mathrm{y}^\top \mathrm{Q}^{-1} \mathrm{y}.$$

Lemma 3. *[37] Let $V(t) \in C([t_0, +\infty), R^+)$ satisfy the fractional differential inequality $\mathcal{D}^\alpha V(t) \leq \varphi V(t)$ for $t > t_0$, where γ is a constant. Then,*

$$V(t) \leq V(t_0) E_\alpha(\varphi(t - t_0)^\alpha), t \geq t_0.$$

Lemma 4. *[37] Let $0 < \alpha < 1$ and $\sigma \leq 0$. The M-L function satisfies $0 \leq E_\alpha(\sigma(t - t_0)^\alpha) \leq 1$ for all $t \geq t_0$ and it is monotonically non-increasing.*

2.3. Model description

Now, we investigate an n-dimensional FOMASs with N nodes, where the system dynamics are characterized by

$$\mathcal{D}^\alpha x_i(t) = (A + \triangle A(t)) x_i(t) + (B + \triangle B(t)) f(x_i(t)) + u_i(t), \tag{2.1}$$

where $i \in \mathbb{I} = \{1, 2, \ldots, N\}$, $\alpha \in (0, 1)$. $x_i(t) \in R^n$ is the state vector; $f(x_i(t)) \in R^n$ is the activation function; $u_i(t)$ represents the control input; A, $B \in R^{n\times n}$ are constant matrices; and $\triangle A(t)$, $\triangle B(t) \in R^{n\times n}$ are uncertain parameter matrices.

For System (2.1), we define the synchronization target system as

$$\mathcal{D}^\alpha x_0(t) = (A + \triangle A(t)) x_0(t) + (B + \triangle B(t)) f(x_0(t)), \tag{2.2}$$

where $x_0(t) \in R^n$.

To approximate the nonlinear systems (2.1) and (2.2), the corresponding TSF models are constructed to describe the dynamics. Under each TSF rule, a local submodel is described in different state space regions. The lth rule of FOMASs (2.1) and (2.2) is respectively represented as
Rule l : IF $\zeta_1(t)$ is M_1^l and $\zeta_2(t)$ is M_2^l and $\cdots$ $\zeta_p(t)$ is M_p^l,
THEN

$$\begin{aligned} \mathcal{D}^\alpha x_i(t) &= (A^l + \triangle A^l(t)) x_i(t) + (B^l + \triangle B^l(t)) f(x_i(t)) + u_i(t) && (2.3) \\ \mathcal{D}^\alpha x_0(t) &= (A^l + \triangle A^l(t)) x_0(t) + (B^l + \triangle B^l(t)) f(x_0(t)), && (2.4) \end{aligned}$$

where $l \in \mathbb{L} = \{1, 2, \ldots, r\}$, and r denotes the total fuzzy rules. $\zeta_m(t)(m = 1, 2, \ldots, p)$ are premise variables, and $M_m^l(m = 1, 2, \ldots, p)$ are their corresponding fuzzy subsets. A^l and $B^l \in R^{n\times n}$ are constant matrices.

The main results are obtained under the following assumption for $\triangle A^l(t)$and $\triangle B^l(t)$:

Assumption 1. *The uncertain parameters $\triangle A^l(t)$ and $\triangle B^l(t)$ are assumed to have the following form:*

$$\triangle A^l(t) = \mathbb{E}_A^l \Phi^l(t) \mathbb{F}_A^l, \triangle B^l(t) = \mathbb{E}_B^l \Phi^l(t) \mathbb{F}_B^l,$$

where $\Phi^l(t)$ is a time-varying uncertainty matrix such that $(\Phi^l(t))^\top \Phi^l(t) \leq I$, and $\mathbb{E}_A^l$, $\mathbb{E}_B^l$, $\mathbb{F}_A^l$, $\mathbb{F}_B^l$ are known constant matrices.

The global TSF systems are synthesized through membership function weighting:

$$\mathcal{D}^\alpha x_i(t) = \sum_{l=1}^{r} h_l(\zeta(t)) \left[(A^l + \triangle A^l(t)) x_i(t) + (B^l + \triangle B^l(t)) f(x_i(t)) + u_i(t) \right], \tag{2.5}$$

$$\mathcal{D}^\alpha x_0(t) = \sum_{l=1}^{r} h_l(\zeta(t)) \left[(A^l + \triangle A^l(t)) x_0(t) + (B^l + \triangle B^l(t)) f(x_0(t)) \right], \tag{2.6}$$

where $\zeta(t) = [\zeta_1(t), \zeta_2(t), \ldots, \zeta_p(t)]$, $h_l(\zeta(t))$ is the normalized membership function with

$$h_l(\zeta(t)) = \frac{\omega^l(\zeta(t))}{\sum_{k=1}^{r} \omega^k(\zeta(t))} \geq 0,$$
$$\omega^l(\zeta(t)) = \prod_{m=1}^{p} M_m^l(\zeta_m(t)), \sum_{l=1}^{r} h_l(\zeta(t)) = 1,$$

where $M_m^l(\zeta_m(t))$ denotes the membership degree of premise variable $\zeta_m(t)$ belonging to fuzzy set M_m^l.

Lemma 5. *Let $h_l \geq 0 (l = 1, 2, \ldots, r)$ be scalar weights satisfying $\sum_{l=1}^{r} h_l = 1$, and let $K_l \in R^{N \times N}$ be any real matrices. Then, the following inequality holds:*

$$(\sum_{l=1}^{r} h_l \mathrm{K}_l)^\top (\sum_{l=1}^{r} h_l \mathrm{K}_l) \leq \sum_{l=1}^{r} h_l \mathrm{K}_l^\top \mathrm{K}_l.$$

Proof. Let $\mathfrak{S} = \sum_{l=1}^{r} h_l \mathrm{K}_l$. Then,

$$\begin{aligned}
\mathfrak{S}^\top \mathfrak{S} &= \sum_{i=1}^{r} \sum_{j=1}^{r} h_i h_j \mathrm{K}_i^\top \mathrm{K}_j \\
&= \sum_{i=1}^{r} h_i^2 \mathrm{K}_i^\top \mathrm{K}_i + \sum_{i=1}^{r} \sum_{j=1, j \neq i}^{r} h_i h_j \mathrm{K}_i^\top \mathrm{K}_j \\
&= \sum_{i=1}^{r} h_i^2 \mathrm{K}_i^\top \mathrm{K}_i + \sum_{i=1}^{r} \sum_{j>i}^{r} h_i h_j (\mathrm{K}_i^\top \mathrm{K}_j + \mathrm{K}_j^\top \mathrm{K}_i).
\end{aligned}$$

Owing to $(\mathrm{K}_i - \mathrm{K}_j)^\top(\mathrm{K}_i - \mathrm{K}_j) \geq 0$, it becomes

$$\begin{aligned}\mathfrak{S}^\top\mathfrak{S} &\leq \sum_{i=1}^{r} h_i^2\mathrm{K}_i^\top\mathrm{K}_i + \sum_{i=1}^{r}\sum_{j>i}^{r} h_ih_j(\mathrm{K}_i^\top\mathrm{K}_i + \mathrm{K}_j^\top\mathrm{K}_j)\\ &= \sum_{i=1}^{r} h_i^2\mathrm{K}_i^\top\mathrm{K}_i + \sum_{i=1}^{r}\sum_{j>i}^{r} h_ih_j\mathrm{K}_i^\top\mathrm{K}_i + \sum_{i=1}^{r}\sum_{j>i}^{r} h_ih_j\mathrm{K}_j^\top\mathrm{K}_j\\ &= \sum_{i=1}^{r} h_i^2\mathrm{K}_i^\top\mathrm{K}_i + \sum_{i=1}^{r} h_i(\sum_{j\neq i}^{r} h_j)\mathrm{K}_i^\top\mathrm{K}_i\\ &= \sum_{l=1}^{r} h_l\mathrm{K}_l^\top\mathrm{K}_l,\end{aligned}$$

where the last equality uses $\sum_{l=1}^{r} h_l = 1$. □

Definition 4. *The exponential consensus between MASs (2.5) and (2.6) is achieved if there exist scalars* $\varrho, \tau, T \in R^+$ *satisfying*

$$\| x_i(t) - x_0(t) \| \leq \varrho e^{-\tau(t-t_0)}, t > T,$$

where τ *characterizes the exponential decay rate.*

Define $\epsilon_i(t) = x_i(t) - x_0(t)$ as the error vector. Subsequently, from (2.5) and (2.6), there is the error system

$$\mathcal{D}^\alpha\epsilon_i(t) = \sum_{l=1}^{r} h_l(\zeta(t))[(A^l + \triangle A^l(t))\epsilon_i(t) + (B^l + \triangle B^l(t))f(\epsilon_i(t)) + u_i(t)], \tag{2.7}$$

in which $f(\epsilon_i(t)) = f(x_i(t)) - f(x_0(t))$.

The exponential consensus of Systems (2.5) and (2.6) under controller $u_i(t)$ means that the error system (2.7) achieves exponential stability.

Make the following assumption for the nonlinear functions f throughout this work:

Assumption 2. *For vectors* $x, y \in R^n$*, there exists diagonal matrix* $L = diag\{l_1, l_2, \ldots, l_n\} > 0$ *such that the nonlinear function* $f(\cdot)$ *satisfies*

$$(x-y)^\top(f(x) - f(y)) \leq (x-y)^\top L(x-y). \tag{2.8}$$

This paper aims to develop a control scheme to ensure exponential consensus achievement for the FOMASs (2.5) and reference system (2.6).

3. Main results

3.1. Leader-following exponential consensus analysis

The impulsive controller for the follower i is constructed as follows to guarantee exponential consensus between systems (2.5) and (2.6):

$$u_i(t) = \rho \sum_{k=1}^{\infty} \delta(t - t_k^-) q_i(t_k), \tag{3.1}$$

where $\rho \in (0, 1)$ denotes the impulsive gain. The impulsive instant sequence $\{t_k, k \in N^+\}$ satisfies that it is increasing, and $\lim_{k\to\infty} t_k = +\infty$, where the interval between adjacent impulses has a lower bound, that is, $t_k - t_{k-1} \geq \theta > 0$. $x(t_k^-)$ and $x(t_k^+)$ respectively represent the left and right limits of the state at the impulsive moment, and $x(t_k) = x(t_k^+)$. Furthermore,

$$q_i(t) = \sum_{j\in N_i} a_{ij}(x_j(t) - x_i(t)) + b_i(x_0(t) - x_i(t)).$$

The impulse controller has the same fuzzy rules as the above system (2.3). Then, the overall fuzzy impulsive control is derived by

$$u_i(t) = \sum_{l=1}^{r} h_l(\zeta(t))\rho_l \sum_{k=1}^{\infty} \delta(t - t_k^-) q_i(t_k). \tag{3.2}$$

Taking (3.2) into (2.7), the error system is rewritten according to [39] as

$$\begin{cases} \mathcal{D}^{\alpha}\epsilon_i(t) = \sum_{l=1}^{r} h_l(\zeta(t))\Big[(A^l + \triangle A^l(t))\epsilon_i(t) + (B^l + \triangle B^l(t)) f(\epsilon_i(t))\Big], t \neq t_k, \\ \epsilon_i(t_k) = \sum_{l=1}^{r} h_l(\zeta(t))\rho_l(\sum_{j\in N_i} a_{ij}(\epsilon_j(t_k^-) - \epsilon_i(t_k^-)) - b_i\epsilon_i(t_k^-)) + \epsilon_i(t_k^-), t = t_k, k \in Z_+. \end{cases} \tag{3.3}$$

Remark 1. *Compared with the traditional fixed-gain impulsive controllers [25], the fuzzy impulsive controller has flexibility in dealing with the nonlinearity and uncertainty in FOMASs. Under the designed TSF impulsive controller, which can adjust the impulsive gain intensity by fuzzy rules, the exponential consensus of uncertain FOMASs is achieved.*

Remark 2. *According to the design of the fuzzy impulsive controller, the impulsive gain ρ_l can be dynamically selected through the current system state, that is, $\zeta(t)$. Furthermore, the design of the controller takes advantage of the inherent low communication frequency characteristic of impulsive control. After integrating fuzzy rules, it can intelligently adjust the impulsive intensity in different system states, thereby further saving energy.*

Theorem 1. *Provided that Assumptions 1 and 2 are valid, if there exist scalars $\varepsilon_1, \varepsilon_2 > 0$, $\mu_l > 0$, $\beta^l < 0$, and $\alpha \in (0, 1]$ and matrices $P, Q > 0$ satisfying the LMIs*

1) $\begin{bmatrix} \Theta_1 & PB^l & 0 & 0 \\ * & -Q & 0 & 0 \\ 0 & 0 & -\mu_l I_N & \Theta_2 \\ 0 & 0 & * & -I_N \end{bmatrix} < 0,$

2) $\mu E_{\alpha}(\beta\theta^{\alpha}) < 1,$

where

$$\Theta_1 = PA^l + (A^l)^{\top}P + L^{\top}QL + \Xi - \beta^l P,$$
$$\Theta_2 = -(I_N - \rho_l(\mathcal{L} + \mathcal{B}))^{\top},$$
$$\Xi = \varepsilon_1 P\mathbb{E}_A^l(\mathbb{E}_A^l)^{\top}P + \varepsilon_1^{-1}(\mathbb{F}_A^l)^{\top}\mathbb{F}_A^l + \varepsilon_2 P\mathbb{E}_B^l(\mathbb{E}_B^l)^{\top}P + \varepsilon_2^{-1}L^T(\mathbb{F}_B^l)^{\top}\mathbb{F}_B^l L,$$

$$\beta = max\{\beta^l\}, \mu = max\{\mu_l\}, l = 1, 2, \ldots, r,$$

then FOMASs (2.5) achieves exponential consensus with the target system (2.6) under the controller (3.2).

Proof. Consider the Lyapunov functional candidate as

$$V(\epsilon(t)) = \sum_{i=1}^{N} \epsilon_i^\top(t) P \epsilon_i(t),$$

and set $V(t) = V(\epsilon(t))$.

For $t \in [t_{k-1}, t_k)$, take the α-order derivative with respect to $V(t)$,

$$\begin{aligned} \mathcal{D}^\alpha V(t) \le& \sum_{i=1}^{N} 2\epsilon_i^\top(t) P \mathcal{D}^\alpha \epsilon_i(t) \\ =& \sum_{i=1}^{N} \sum_{l=1}^{r} h_l(\zeta(t)) \Big[\epsilon_i^\top(t)(PA^l + (A^l)^\top P)\epsilon_i(t) + 2\epsilon_i^\top(t) P \triangle A^l(t) \epsilon_i(t) \\ &+ 2\epsilon_i^\top(t) P (B^l + \triangle B^l(t)) f(\epsilon_i(t)) \Big]. \end{aligned} \tag{3.4}$$

Combining Lemma 2 with Assumption 1 yields

$$\begin{aligned} 2\epsilon_i^\top(t) P \triangle A^l(t) \epsilon_i(t) =& 2\epsilon_i^\top(t) P \mathbb{E}_A^l \Phi^l(t) \mathbb{F}_A^l \epsilon_i(t) \\ \le& \varepsilon_1 \epsilon_i^\top(t) P \mathbb{E}_A^l \Phi^l(t) (\Phi^l(t))^\top (\mathbb{E}_A^l)^\top P \epsilon_i(t) + \varepsilon_1^{-1} \epsilon_i^\top(t) (\mathbb{F}_A^l)^\top \mathbb{F}_A^l \epsilon_i(t) \\ \le& \epsilon_i^\top(t) \left(\varepsilon_1 P \mathbb{E}_A^l (\mathbb{E}_A^l)^\top P + \varepsilon_1^{-1} (\mathbb{F}_A^l)^\top \mathbb{F}_A^l \right) \epsilon_i(t). \end{aligned} \tag{3.5}$$

By Assumption 2, the following holds:

$$\begin{aligned} 2\epsilon_i^\top(t) P B^l f(\epsilon_i(t)) \le& \epsilon_i^\top(t) P B^l Q^{-1} (B^l)^\top P \epsilon_i(t) + f^\top(\epsilon_i(t)) Q f(\epsilon_i(t)) \\ \le& \epsilon_i^\top(t) P B^l Q^{-1} (B^l)^\top P \epsilon_i(t) + \epsilon_i^\top(t) L^\top Q L \epsilon_i(t) \\ =& \epsilon_i^\top(t) (P B^l Q^{-1} (B^l)^\top P + L^\top Q L) \epsilon_i(t). \end{aligned} \tag{3.6}$$

Similarly,

$$\begin{aligned} 2\epsilon_i^\top(t) P \triangle B^l(t) f(\epsilon_i(t)) =& 2\epsilon_i^\top(t) P \mathbb{E}_B^l \Phi^l(t) \mathbb{F}_B^l f(\epsilon_i(t)) \\ \le& \varepsilon_2 \epsilon_i^\top(t) P \mathbb{E}_B^l (\mathbb{E}_B^l)^\top P \epsilon_i(t) + \varepsilon_2^{-1} \epsilon_i^\top(t) L^\top (\mathbb{F}_B^l)^\top \mathbb{F}_B^l L \epsilon_i(t) \\ =& \epsilon_i^\top(t) (\varepsilon_2 P \mathbb{E}_B^l (\mathbb{E}_B^l)^\top P + \varepsilon_2^{-1} L^\top (\mathbb{F}_B^l)^\top \mathbb{F}_B^l L) \epsilon_i(t). \end{aligned} \tag{3.7}$$

Substituting (3.5), (3.6), and (3.7) into (3.4) leads to

$$\begin{aligned} \mathcal{D}^\alpha V(t) \le& \sum_{i=1}^{N} \sum_{l=1}^{r} h_l(\zeta(t)) \Big[\epsilon_i^\top(t)(PA^l + (A^l)^\top P + P B^l Q^{-1} (B^l)^\top P + L^\top Q L + \Xi) \epsilon_i(t) \Big] \\ <& \sum_{i=1}^{N} \sum_{l=1}^{r} h_l(\zeta(t)) (\epsilon_i^\top(t) (\beta^l P) \epsilon_i(t)) \\ \le& \sum_{i=1}^{N} \sum_{l=1}^{r} \beta h_l(\zeta(t)) \epsilon_i^\top(t) P \epsilon_i(t) \\ =& \beta V(t), t \in [t_{k-1}, t_k). \end{aligned} \tag{3.8}$$

According to Lemma 3 and Inequality (3.8), it has

$$V(t) \leq V(t_{k-1})E_\alpha(\beta(t - t_{k-1})^\alpha). \tag{3.9}$$

Moreover, one can obtain from error system (3.3) that at $t = t_k$,

$$\begin{aligned} V(t_k) &= \sum_{i=1}^{N} \epsilon_i^\top(t_k)P\epsilon_i(t_k) \\ &= \sum_{i=1}^{N} \Big[\sum_{l=1}^{r} h_l(\zeta(t))\rho_l(\sum_{j\in N_i} a_{ij}(\epsilon_j^\top(t_k^-) - \epsilon_i^\top(t_k^-)) - b_i\epsilon_i^\top(t_k^-)) + \epsilon_i^\top(t_k^-)\Big]P \\ &\quad \Big[\sum_{l=1}^{r} h_l(\zeta(t))\rho_l\Big(\sum_{j\in N_i} a_{ij}(\epsilon_j(t_k^-) - \epsilon_i(t_k^-)) - b_i\epsilon_i(t_k^-)\Big) + \epsilon_i(t_k^-)\Big]. \end{aligned} \tag{3.10}$$

Define vector

$$w_i = \left[a_{i1}, \cdots, a_{i(i-1)}, -b_i - \sum_{j\in N_i}^{N} a_{ij}, a_{i(i+1)}, \cdots, a_{iN} \right]^\top$$

and matrix $W = \begin{bmatrix} w_1 & w_2 & \ldots & w_N \end{bmatrix}^\top = -(\mathcal{L} + \mathcal{B})$. For each agent i, we have $\sum_{j\in N_i} a_{ij}(\epsilon_j(t_k^-) - \epsilon_i(t_k^-)) - b_i\epsilon_i(t_k^-) = (w_i^\top \otimes I_n)\epsilon(t_k^-)$, where $\epsilon(t) = (\epsilon_1^\top(t), \epsilon_2^\top(t), \ldots, \epsilon_N^\top(t))^\top$. Then, the compact form of the error system at $t = t_k$ can be reformulated as $\epsilon(t_k) = (I_N - \sum_{l=1}^{r} h_l(\zeta(t))\rho_l(\mathcal{L} + \mathcal{B})) \otimes I_n\epsilon(t_k^-) = \Delta \otimes I_n\epsilon(t_k^-)$, where $\Delta = I_N - \sum_{l=1}^{r} h_l(\zeta(t))\rho_l(\mathcal{L} + \mathcal{B})$. Incorporating the properties of the Kronecker product yields

$$\begin{aligned} V(t_k) =&\epsilon^\top(t_k)(I_N \otimes P)\epsilon(t_k) \\ =&\epsilon^\top(t_k^-)[(\Delta^\top\Delta) \otimes P]\epsilon(t_k^-). \end{aligned} \tag{3.11}$$

In light of Lemma 5, we deduce

$$\begin{aligned} \Delta^\top\Delta &= (\sum_{l=1}^{r} h_l(\zeta(t))(I_N - \rho_l(\mathcal{L} + \mathcal{B})))^\top(\sum_{l=1}^{r} h_l(\zeta(t))(I_N - \rho_l(\mathcal{L} + \mathcal{B}))) \\ &\leq \sum_{l=1}^{r} h_l(\zeta(t))(I_N - \rho_l(\mathcal{L} + \mathcal{B}))^\top(I_N - \rho_l(\mathcal{L} + \mathcal{B})). \end{aligned} \tag{3.12}$$

Therefore, (3.11) can be reduced to

$$\begin{aligned} V(t_k) &\leq \epsilon^\top(t_k^-)\Big[\Big(\sum_{l=1}^{r} h_l(\zeta(t))(I_N - \rho_l(\mathcal{L} + \mathcal{B}))^\top(I_N - \rho_l(\mathcal{L} + \mathcal{B}))\Big) \otimes P\Big]\epsilon(t_k^-) \\ &< \sum_{l=1}^{r} h_l(\zeta(t))\epsilon^\top(t_k^-)[(\mu_l I_N) \otimes P]\epsilon(t_k^-) \\ &\leq \sum_{l=1}^{r} h_l(\zeta(t))\mu\epsilon^\top(t_k^-)(I_N \otimes P)\epsilon(t_k^-) \\ &= \mu V(t_k^-). \end{aligned} \tag{3.13}$$

For all $k \in N^+$, combining (3.9) with (3.13) yields

$$V(t_k) \leq \mu V(t_{k-1}) E_\alpha(\beta(t_k^- - t_{k-1})^\alpha).$$

Hence, by employing the method of induction, we have

$$\begin{aligned} V(t_k) \leq& \mu^2 V(t_{k-2}) E_\alpha(\beta(t_{k-1}^- - t_{k-2})^\alpha) E_\alpha(\beta(t_k^- - t_{k-1})^\alpha) \\ \leq& \mu^k V(t_0) E_\alpha(\beta(t_1^- - t_0)^\alpha) \cdots E_\alpha(\beta(t_{k-1}^- - t_{k-2})^\alpha) E_\alpha(\beta(t_k^- - t_{k-1})^\alpha) \\ =& \mu^k V(t_0) \prod_{i=1}^{k} E_\alpha(\beta(t_i^- - t_{i-1})^\alpha). \end{aligned} \tag{3.14}$$

For all $t > t_0$, one can find $k \in N^+$ ensuring t lies in the impulsive interval $[t_k, t_{k+1})$. From (3.9), (3.14), and Lemma 4, we obtain

$$\begin{aligned} V(t) \leq& V(t_k) E_\alpha(\beta(t - t_k)^\alpha) \\ \leq& \mu^k V(t_0) \prod_{i=1}^{k} E_\alpha(\beta(t_i^- - t_{i-1})^\alpha) E_\alpha(\beta(t - t_k)^\alpha) \\ \leq& V(t_0)(\mu E_\alpha(\beta\theta^\alpha))^k. \end{aligned} \tag{3.15}$$

In addition, there exists a nonnegative number $\mathbb{N}_0$ such that $(t - t_0)/T_a - \mathbb{N}_0 \leq k \leq (t - t_0)/T_a + \mathbb{N}_0$. From Condition 2 in Theorem 1, it follows that

$$\begin{aligned} V(t) \leq& V(t_0)(\mu E_\alpha(\beta\theta^\alpha))^{-\mathbb{N}_0} (\mu E_\alpha(\beta\theta^\alpha))^{\frac{t-t_0}{T_a}} \\ =& V(t_0) M e^{\frac{ln(\mu E_\alpha(\beta\theta^\alpha))}{T_a}(t-t_0)}, \end{aligned} \tag{3.16}$$

where $M = (\mu E_\alpha(\beta\theta^\alpha))^{-\mathbb{N}_0} > 0$.

Meanwhile, we can get

$$V(t) \geq \lambda_{min}(P) \|\epsilon(t)\|^2.$$

Then, we can conclude that

$$\|\epsilon(t)\| \leq G e^{\frac{ln(\mu E_\alpha(\beta\theta^\alpha))}{T_a}(t-t_0)}, t > t_0,$$

where $G = \sqrt{\frac{V(t_0)M}{\lambda_{min}(P)}}$.

By Definition 4, the exponential consensus of FOMASs (2.5) and (2.6) is guaranteed. □

Remark 3. *For the conditions in Theorem 1, by applying the Schur complement lemma, the LMIs are linear with respect to the variables. The procedure for constructing LMIs for the given system is standard and can be solved using professional tools. As the number of agents and fuzzy rules increases, the scale of LMIs also grows. Nevertheless, the intrinsic sparsity of the LMIs, characterized by numerous zero elements, renders the computation tractable when N and l are within reasonable ranges.*

3.2. Leaderless exponential consensus analysis

To derive the consensus result, we define $\bar{x}(t) = (1/N)\sum_{i=1}^{N} x_i(t)$. From (2.5), we obtain

$$\mathcal{D}^{\alpha}\bar{x}(t) = \sum_{l=1}^{r} h_l(\zeta(t))\Big[(A^l + \triangle A^l(t))\bar{x}(t) + (B^l + \triangle B^l(t))\frac{1}{N}\sum_{m=1}^{N} f(x_m(t)) + \frac{1}{N}\sum_{m=1}^{N} u_m(t)\Big]. \tag{3.17}$$

Notice that at $\bar{\epsilon}_i(t) = x_i(t) - \bar{x}(t)$, one gets

$$\begin{aligned}\mathcal{D}^{\alpha}\bar{\epsilon}_i(t) = \sum_{l=1}^{r} h_l(\zeta(t))\Big[&(A^l + \triangle A^l(t))\bar{\epsilon}_i(t) + (B^l + \triangle B^l(t))(f(x_i(t)) - \frac{1}{N}\sum_{m=1}^{N} f(x_m(t)))\\ &+ u_i(t) - \frac{1}{N}\sum_{m=1}^{N} u_m(t)\Big].\end{aligned} \tag{3.18}$$

To achieve leaderless consensus, we use the following control protocol:

$$u_i(t) = \sum_{l=1}^{r} h_l(\zeta(t))\rho_l \sum_{k=1}^{\infty}\delta(t - t_k^-)(\sum_{j\in N_i} a_{ij}(x_j(t) - x_i(t))). \tag{3.19}$$

Moreover, it is not difficult to obtain that

$$\begin{cases}\mathcal{D}^{\alpha}\bar{\epsilon}_i(t) = \sum_{l=1}^{r} h_l(\zeta(t))\Big[(A^l + \triangle A^l(t))\bar{\epsilon}_i(t) + (B^l + \triangle B^l(t))f(\bar{\epsilon}_i(t))\Big], t \neq t_k,\\ \bar{\epsilon}_i(t) = \sum_{l=1}^{r} h_l(\zeta(t))\rho_l(\sum_{j\in N_i} a_{ij}(\bar{\epsilon}_j(t^-) - \bar{\epsilon}_i(t^-))) - \frac{1}{N}\sum_{m=1}^{N}\sum_{l=1}^{r} h_l(\zeta(t))\rho_l\\ \quad (\sum_{j\in N_m} a_{mj}(\bar{\epsilon}_j(t^-) - \bar{\epsilon}_m(t^-))) + \bar{\epsilon}_i(t^-), t = t_k, k \in Z_+,\end{cases} \tag{3.20}$$

where $f(\bar{\epsilon}_i(t)) = f(x_i(t)) - (1/N)\sum_{m=1}^{N} f(x_m(t))$. To simplify the expression of the error system, following a procedure similar to the proof of Theorem 1, we introduce two new quantities, $\psi = [\sum_{j=1}^{N} l_{j1}, \sum_{j=1}^{N} l_{j2}, \cdots, \sum_{j=1}^{N} l_{jN}]^{\top}$ and $\Psi = \begin{bmatrix}\psi & \psi & \dots & \psi\end{bmatrix}^{\top}$.

Theorem 2. *Provided that Assumptions 1 and 2 are valid, if there exist scalars $\varepsilon_3, \varepsilon_4 > 0$, $\bar{\mu}_l > 0$, $\bar{\beta}^l < 0$, and $\alpha \in (0, 1]$ and matrices $P, R > 0$ satisfying the LMIs*

1) $\begin{bmatrix}\Theta_3 & PB^l & 0 & 0\\ * & -R & 0 & 0\\ 0 & 0 & -\bar{\mu}_l I_N & \Theta_4\\ 0 & 0 & * & -I_N\end{bmatrix} < 0$

2) $\bar{\mu}E_{\alpha}(\bar{\beta}\theta^{\alpha}) < 1$

where

$$\Theta_3 = PA^l + (A^l)^{\top}P + L^{\top}RL + \Lambda - \bar{\beta}^l P,$$

$$\Theta_4 = -(I_N - \rho_l(\mathcal{L} - \frac{1}{N}\Psi))^{\top},$$

$$\Lambda = \varepsilon_3 P\mathbb{E}_A^l(\mathbb{E}_A^l)^{\top}P + \varepsilon_3^{-1}(\mathbb{F}_A^l)^{\top}\mathbb{F}_A^l + \varepsilon_4 P\mathbb{E}_B^l(\mathbb{E}_B^l)^{\top}P + \varepsilon_4^{-1}L^{\top}(\mathbb{F}_B^l)^{\top}\mathbb{F}_B^l L,$$

$$\bar{\beta} = max\{\bar{\beta}^l\}, \bar{\mu} = max\{\bar{\mu}_l\}, l = 1, 2, \dots, r,$$

$$\Psi = \begin{bmatrix} \sum_{j=1}^{N} l_{j1} & \sum_{j=1}^{N} l_{j2} & \cdots & \sum_{j=1}^{N} l_{jN} \\ \sum_{j=1}^{N} l_{j1} & \sum_{j=1}^{N} l_{j2} & \cdots & \sum_{j=1}^{N} l_{jN} \\ \vdots & \vdots & & \vdots \\ \sum_{j=1}^{N} l_{j1} & \sum_{j=1}^{N} l_{j2} & \cdots & \sum_{j=1}^{N} l_{jN} \end{bmatrix},$$

then FOMASs (2.5) achieves exponential consensus under the controller (3.19).

Proof. Similar to Theorem 1, we choose the positive definite Lyapunov functional as

$$\bar{V}(t) = \sum_{i=1}^{N} \bar{\epsilon}_i^\top(t) P \bar{\epsilon}_i(t).$$

Then, taking the α order derivative of $\bar{V}(t)$ about t yields

$$\begin{aligned} \mathscr{D}^\alpha \bar{V}(t) \leq \sum_{i=1}^{N} \sum_{l=1}^{r} h_l(\zeta(t)) \Big[& \bar{\epsilon}_i^\top(t)(PA^l + (A^l)^\top P)\bar{\epsilon}_i(t) + 2\bar{\epsilon}_i^\top(t) P \triangle A^l(t) \bar{\epsilon}_i(t) \\ & + 2\bar{\epsilon}_i^\top(t) P(B^l + \triangle B^l(t)) f(\bar{\epsilon}_i(t)) \Big]. \end{aligned} \tag{3.21}$$

Then, by Lemma 2, one has

$$2\bar{\epsilon}_i^\top(t) P \triangle A^l(t) \bar{\epsilon}_i(t) \leq \bar{\epsilon}_i^\top(t)(\varepsilon_3 P \mathbb{E}_A^l (\mathbb{E}_A^l)^\top P + \varepsilon_3^{-1} (\mathbb{F}_A^l)^\top \mathbb{F}_A^l) \bar{\epsilon}_i(t). \tag{3.22}$$

According to our assumptions, we obtain

$$\begin{aligned} 2\bar{\epsilon}_i^\top(t) P B^l f(\bar{\epsilon}_i(t)) &\leq \bar{\epsilon}_i^\top(t) P B^l R^{-1} (B^l)^\top P \bar{\epsilon}_i(t) + f^\top(\bar{\epsilon}_i(t)) R f(\bar{\epsilon}_i(t)) \\ &\leq \bar{\epsilon}_i^\top(t) P B^l R^{-1} (B^l)^\top P \bar{\epsilon}_i(t) + \bar{\epsilon}_i^\top(t) L^\top R L \bar{\epsilon}_i(t) \\ &= \bar{\epsilon}_i^\top(t)(P B^l R^{-1} (B^l)^\top P + L^\top R L) \bar{\epsilon}_i(t) \end{aligned} \tag{3.23}$$

and

$$\begin{aligned} 2\bar{\epsilon}_i^\top(t) P \triangle B^l(t) f(\bar{\epsilon}_i(t)) &\leq \varepsilon_4 \bar{\epsilon}_i^\top(t) P \mathbb{E}_B^l (\mathbb{E}_B^l)^\top P \bar{\epsilon}_i(t) + \varepsilon_4^{-1} \bar{\epsilon}_i^\top(t) L^\top (\mathbb{F}_B^l)^\top \mathbb{F}_B^l L \bar{\epsilon}_i(t) \\ &= \bar{\epsilon}_i^\top(t)(\varepsilon_4 P \mathbb{E}_B^l (\mathbb{E}_B^l)^\top P + \varepsilon_4^{-1} L^\top (\mathbb{F}_B^l)^\top \mathbb{F}_B^l L) \bar{\epsilon}_i(t). \end{aligned} \tag{3.24}$$

Based on (3.21)–(3.24), the following inequality is obtained:

$$\begin{aligned} \mathscr{D}^\alpha \bar{V}(t) &\leq \sum_{i=1}^{N} \sum_{l=1}^{r} h_l(\zeta(t)) \Big[\bar{\epsilon}_i^\top(t)(PA^l + (A^l)^\top P + P B^l R^{-1} (B^l)^\top P + L^\top R L + \Lambda) \bar{\epsilon}_i(t) \Big] \\ &< \sum_{i=1}^{N} \sum_{l=1}^{r} h_l(\zeta(t))(\bar{\epsilon}_i^\top(t)(\bar{\beta}^l P) \bar{\epsilon}_i(t)) \\ &\leq \sum_{i=1}^{N} \sum_{l=1}^{r} \bar{\beta} h_l(\zeta(t)) \bar{\epsilon}_i^\top(t) P \bar{\epsilon}_i(t) \\ &= \bar{\beta} \bar{V}(t), t \in [t_{k-1}, t_k). \end{aligned} \tag{3.25}$$

At the impulsive instants $t = t_k$, the Lyapunov function satisfies

$$
\begin{aligned}
\bar{V}(t_k) &= \sum_{i=1}^{N} \bar{\epsilon}_i^\top(t_k)P\bar{\epsilon}_i(t_k) \\
&= \sum_{i=1}^{N}\Big[\sum_{l=1}^{r} h_l(\zeta(t))\rho_l\Big(\sum_{j\in N_i} a_{ij}(\bar{\epsilon}_j^\top(t_k^-) - \bar{\epsilon}_i^\top(t_k^-))\Big) - \frac{1}{N}\sum_{m=1}^{N}\sum_{l=1}^{r} h_l(\zeta(t))\rho_l \\
&\quad \Big(\sum_{j\in N_m} a_{mj}(\bar{\epsilon}_j^\top(t_k^-) - \bar{\epsilon}_m^\top(t_k^-))\Big) + \bar{\epsilon}_i^\top(t_k^-)\Big]P\Big[\sum_{l=1}^{r} h_l(\zeta(t))\rho_l\Big(\sum_{j\in N_i} a_{ij}(\bar{\epsilon}_j(t_k^-) - \bar{\epsilon}_i(t_k^-))\Big) \\
&\quad - \frac{1}{N}\sum_{m=1}^{N}\sum_{l=1}^{r} h_l(\zeta(t))\rho_l\Big(\sum_{j\in N_m} a_{mj}(\bar{\epsilon}_j(t_k^-) - \bar{\epsilon}_m(t_k^-))\Big) + \bar{\epsilon}_i(t_k^-)\Big].
\end{aligned}
\tag{3.26}
$$

Similar to Theorem 1, $(1/N)\sum_{m=1}^{N}\big(\sum_{j\in N_m} a_{mj}(\bar{\epsilon}_j(t_k^-) - \bar{\epsilon}_m(t_k^-))\big) = -(1/N)(A\otimes I_n)\bar{\epsilon}(t_k^-)$. Consequently, the error system can be reformulated as $\bar{\epsilon}(t_k) = \big(I_N - \sum_{l=1}^{r} h_l(\zeta(t))\rho_l(\mathcal{L} - (1/N)\Psi)\big)\otimes I_n\,\bar{\epsilon}(t_k^-)$. For convenience, the above formula is written as a Kronecker product:

$$
\begin{aligned}
\bar{V}(t_k) =& \bar{\epsilon}^\top(t_k^-)\Big[\Big((I_N - \sum_{l=1}^{r} h_l(\zeta(t))\rho_l(\mathcal{L} - \frac{1}{N}\Psi))^\top(I_N - \sum_{l=1}^{r} h_l(\zeta(t))\rho_l(\mathcal{L} - \frac{1}{N}\Psi))\Big)\otimes P\Big]\bar{\epsilon}(t_k^-) \\
\le& \bar{\epsilon}^\top(t_k^-)\Big[\Big(\sum_{l=1}^{r} h_l(\zeta(t))(I_N - \rho_l(\mathcal{L} - \frac{1}{N}\Psi))^\top(I_N - \rho_l(\mathcal{L} - \frac{1}{N}\Psi))\Big)\otimes P\Big]\bar{\epsilon}(t_k^-) \\
<& \sum_{l=1}^{r} h_l(\zeta(t))\bar{\epsilon}^\top(t_k^-)[(\bar{\mu}_l I_N)\otimes P]\bar{\epsilon}(t_k^-) \\
\le& \sum_{l=1}^{r} h_l(\zeta(t))\bar{\mu}\bar{\epsilon}^\top(t_k^-)(I_N\otimes P)\bar{\epsilon}(t_k^-) \\
=& \bar{\mu}\bar{V}(t_k^-).
\end{aligned}
\tag{3.27}
$$

The remainder of the proof follows analogous procedures to Theorem 1 and is omitted for simplicity. □

4. An application example

Consider a two-dimensional fractional-order MASs with five nodes. The communication connection of leader and followers is displayed in Figure 1, which is the directed graph. The blue-highlighted 0 represents the leader agent, and the others are followers.

Specifically, the dynamical model for each agent is represented by a single-link manipulator, as shown in Figure 2, with the following equations:

$$
p\mathcal{D}^{2\alpha}\theta(t) + q\mathcal{D}^{\alpha}\theta(t) + mgl\sin(\theta(t)) = \tau(t), \tag{4.1}
$$

and the specific physical meanings of variables in system (4.1) are presented in the Table 2.

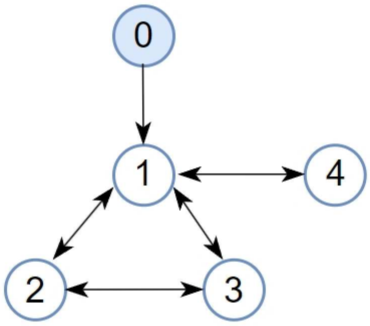

Figure 1. Communication topology graph.

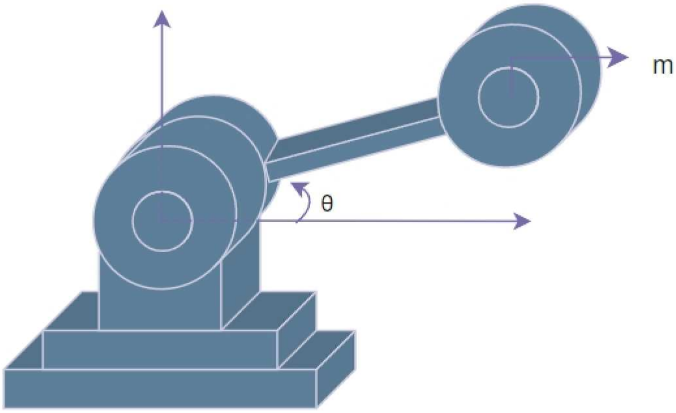

Figure 2. Diagram of one-link manipulator.

Denote $x(t) = (x_1(t), x_2(t))^\top$, $x_1(t) = \theta(t)$, $x_2(t) = \mathcal{D}^\alpha \theta(t)$. Then, (4.1) can be reconstructed as

$$\mathcal{D}^\alpha x(t) = \mathbb{M}x(t) + \mathbb{N}f(x(t)) + \begin{bmatrix} 0 \\ \frac{\tau(t)}{p} \end{bmatrix}, \tag{4.2}$$

where

$$\mathbb{M} = \begin{bmatrix} 0 & 1 \\ 0 & -\frac{q}{p} \end{bmatrix}, \mathbb{N} = \begin{bmatrix} 0 & 0 \\ 0 & -\frac{mgl}{p} \end{bmatrix}, f(x(t)) = \begin{bmatrix} 0 \\ \sin(x_1(t)) \end{bmatrix}.$$

In fact, parameters such as the damping coefficient q and the gravitational acceleration g are not entirely accurate and may vary due to temperature or operating conditions. To simulate this situation, we introduce uncertainties $\triangle\mathbb{M}(t)$ and $\triangle\mathbb{N}(t)$ with structures $\mathbb{E}_\mathbb{M}\Phi(t)\mathbb{F}_\mathbb{M}$ and $\mathbb{E}_\mathbb{N}\Phi(t)\mathbb{F}_\mathbb{N}$ in system (4.2).

Table 2. Model parameters and their physical meanings

Symbol	Represents
$\theta(t)$	Angular displacement of the manipulator joint
$\mathcal{D}^{\alpha}\theta(t)$	Angular velocity of the manipulator joint
$\mathcal{D}^{2\alpha}\theta(t)$	Angular acceleration of the manipulator joint
p	Moment of inertia
q	Damping coefficient
m	Mass of the manipulator
l	Length of the single-link manipulator
g	Gravitational acceleration
$\tau(t)$	Control torque applied to joints

Then, the single-link robotic manipulator model is reformulated as

$$\mathcal{D}^{\alpha}x(t) = (\mathbb{M} + \triangle\mathbb{M}(t))x(t) + (\mathbb{N} + \triangle\mathbb{N}(t))f(x(t)) + \begin{bmatrix} 0 \\ \frac{\tau(t)}{p} \end{bmatrix}. \tag{4.3}$$

For each fuzzy rule, the TSF model of the leader and the ith follower are expressed as follows:
Rule 1: IF $\zeta_1(t)$ is M_1^1, and $\zeta_2(t)$ is M_2^1,
THEN

$$\begin{aligned}\mathcal{D}^{\alpha}x_0(t) &= (\mathbb{M}^1 + \triangle\mathbb{M}^1(t))x_0(t) + (\mathbb{N}^1 + \triangle\mathbb{N}^1(t))f(x_0(t)),\\ \mathcal{D}^{\alpha}x_i(t) &= (\mathbb{M}^1 + \triangle\mathbb{M}^1(t))x_i(t) + (\mathbb{N}^1 + \triangle\mathbb{N}^1(t))f(x_i(t)) + u_i(t).\end{aligned}$$

Rule 2: IF $\zeta_1(t)$ is M_1^2, and $\zeta_2(t)$ is M_2^2,
THEN

$$\begin{aligned}\mathcal{D}^{\alpha}x_0(t) &= (\mathbb{M}^2 + \triangle\mathbb{M}^2(t))x_0(t) + (\mathbb{N}^2 + \triangle\mathbb{N}^2(t))f(x_0(t)),\\ \mathcal{D}^{\alpha}x_i(t) &= (\mathbb{M}^2 + \triangle\mathbb{M}^2(t))x_i(t) + (\mathbb{N}^2 + \triangle\mathbb{N}^2(t))f(x_i(t)) + u_i(t),\end{aligned}$$

where $\triangle\mathbb{M}^l(t) = \mathbb{E}_{\mathbb{M}}^l\Phi^l(t)\mathbb{F}_{\mathbb{M}}^l$, $\triangle\mathbb{N}^l(t) = \mathbb{E}_{\mathbb{N}}^l\Phi^l(t)\mathbb{F}_{\mathbb{N}}^l$, and $(\Phi^l(t))^{\top}\Phi^l(t) \leq I$, $l = 1, 2$.

The fuzzy weighting functions are constructed as $h_1(t) = \sin^2 t$ and $h_2(t) = \cos^2 t$. The nonlinear function in the system (4.3) satisfies Assumption 2, where $L = diag\{1/2, 1/2\}$. With $\alpha = 0.8$, the system parameters are given as follows:

$$\mathbb{M}^1 = \begin{bmatrix} 0 & 1 \\ 0 & -0.1 \end{bmatrix}, \mathbb{M}^2 = \begin{bmatrix} 0 & 1 \\ 0 & -0.2 \end{bmatrix},$$

$$\mathbb{N}^1 = \begin{bmatrix} 0 & 0 \\ 0 & -0.7 \end{bmatrix}, \mathbb{N}^2 = \begin{bmatrix} 0 & 0 \\ 0 & -1.4 \end{bmatrix},$$

$$\mathbb{E}_{\mathbb{M}}^1 = \mathbb{E}_{\mathbb{M}}^2 = \begin{bmatrix} 0.2 & 0 \\ 0 & 0.2 \end{bmatrix}, \mathbb{F}_{\mathbb{M}}^1 = \mathbb{F}_{\mathbb{M}}^2 = \begin{bmatrix} 0.2 & 0 \\ 0 & 0.2 \end{bmatrix},$$

$$\mathbb{E}_{\mathbb{N}}^1 = \mathbb{E}_{\mathbb{N}}^2 = \begin{bmatrix} 0.3 & 0 \\ 0 & 0.3 \end{bmatrix}, \mathbb{F}_{\mathbb{N}}^1 = \mathbb{F}_{\mathbb{N}}^2 = \begin{bmatrix} 0.3 & 0 \\ 0 & 0.3 \end{bmatrix},$$

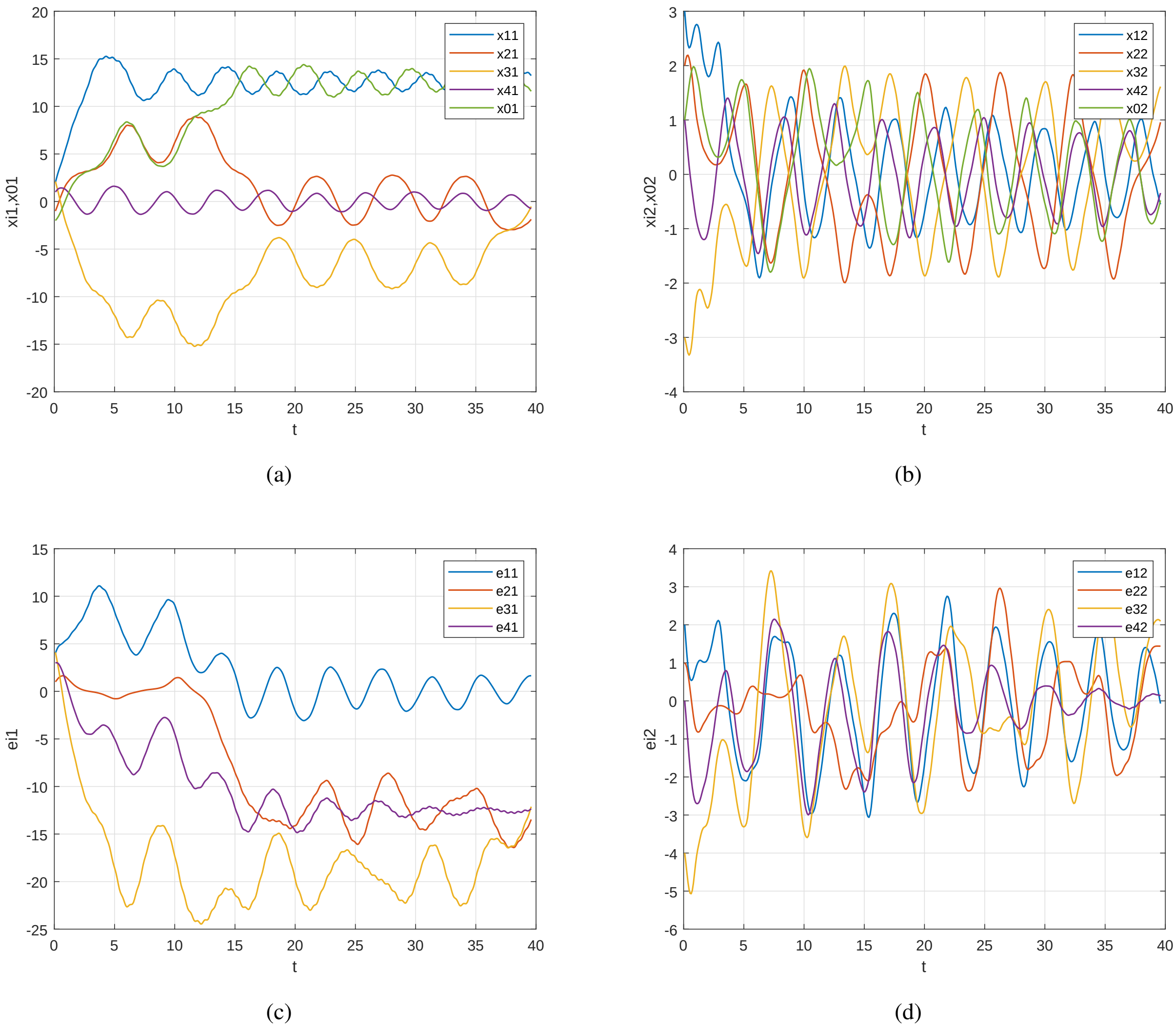

Figure 3. Without Controller case: (a) System state $x_{i1}(t)$ and $x_{01}(t)$; (b) System state $x_{i2}(t)$ and $x_{02}(t)$; (c) The evolution of tracking error $\epsilon_{i1}(t)$; (d) The evolution of tracking error $\epsilon_{i2}(t)(i = 1, 2, 3, 4)$.

$$\Phi^1(t) = \Phi^2(t) = \begin{bmatrix} \sin(t) & 0 \\ 0 & \cos(t) \end{bmatrix}.$$

The initial values are selected as $x_0(0) = (-2, 1)^\top$, $x_1(0) = (2, 3)^\top$, $x_2(0) = (-1, 2)^\top$, $x_3(0) = (2.1, -3)^\top$, $x_4(0) = (1, 1)^\top$. It is evident that the leader-follower consensus cannot be attained in the absence of the controller $u_i(t)$ from Figure 3. According to Theorem 1, proper parameters $\varepsilon_1 = \varepsilon_2 = 2.1161$, $\mu = 2.3468$, and $\beta = -2.1161$ and positive-definite matrices P and Q,

$$P = \begin{bmatrix} 0.7774 & 0.1299 \\ 0.1299 & 0.5966 \end{bmatrix}, Q = \begin{bmatrix} 1.4445 & -0.1556 \\ -0.1556 & 2.0871 \end{bmatrix}.$$

The controller gains $\rho_1 = 0.300$, $\rho_2 = 0.400$ are selected to satisfy Conditions 1 and 2 in Theorem 1. The impulsive sequence is chosen as follows: $\{t_k\}$={0.2,0.77,1.2,2.5,3.4,4}. In addition, for the given

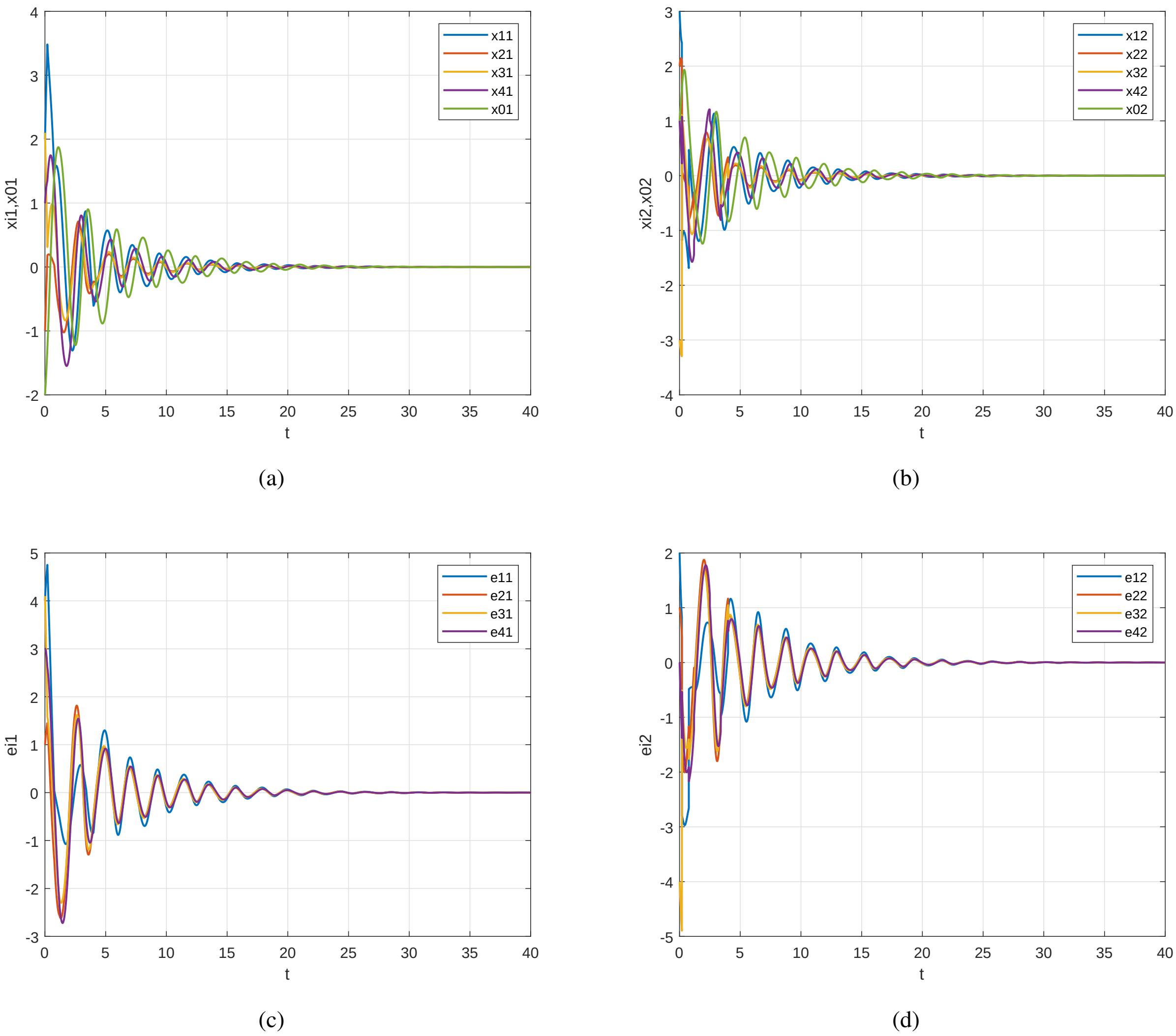

Figure 4. Under Controller $u_i(t)$ case: (a) System state $x_{i1}(t)$ and $x_{01}(t)$; (b) System state $x_{i2}(t)$ and $x_{02}(t)$; (c) The evolution of tracking error $\epsilon_{i1}(t)$; (d) The evolution of tracking error $\epsilon_{i2}(t)(i = 1, 2, 3, 4)$.

μ and β, the formula $\mu E_\alpha(\beta\theta^\alpha) = 0.8957 < 1$ satisfies Theorem 1. Under the impulsive control, the trajectories of leader agent x_{0j} and followers x_{ij}, $i = 1, 2, 3, 4$, $j = 1, 2$ of system (4.3) are shown in Figure 4(a),(b). Moreover, the evolution of errors $\epsilon_{ij} = x_{ij} - x_{0j}$, $i = 1, 2, 3, 4$, $j = 1, 2$ are given in Figure 4(c),(d). In Figure 4, the synchronization errors ϵ_{ij} tend to zero over time, demonstrating that systems (4.3) can achieve exponential consensus under the controller (3.2).

In order to visualize the advantages of the proposed TSF impulsive controller, we compare it with the traditional fixed gain impulsive controller. Figures 5–6 depict the evolution of the states $x_{i1}(t)$ and $x_{01}(t)$ with fixed gains $\rho_{fixed} = 0.355$, $\rho_{fixed} = 0.435$, respectively. The results intuitively demonstrate the superior convergence speed of the proposed TSF impulsive control strategy.

To investigate the impact of fractional order on consensus performance, we adjust the value of α while keeping all other parameters unchanged. Figures 7–8 describe the evolution of system state $x_{i1}(t)$

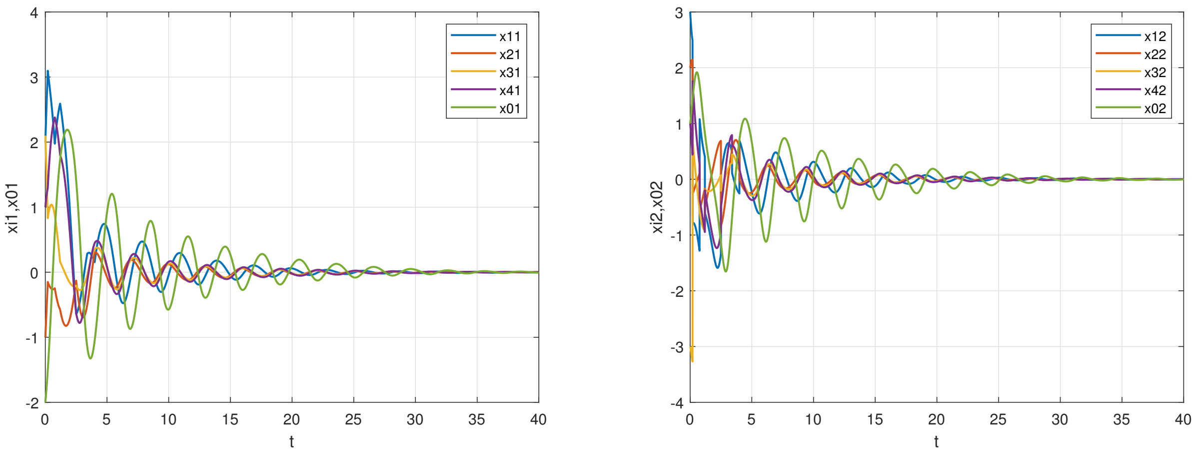

(a) (b)

Figure 5. The evolution of system state $x_{i1}(t)$ and $x_{i2}(t)(i = 0, 1, 2, 3, 4)$ with the fixed gain $\rho_{fixed} = 0.355$.

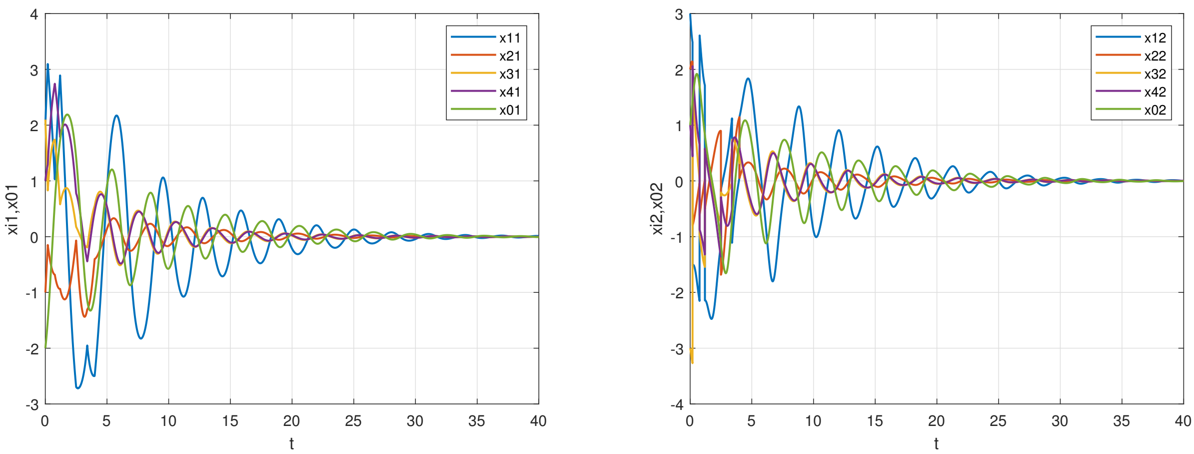

(a) (b)

Figure 6. The evolution of system state $x_{i1}(t)$ and $x_{i2}(t)(i = 0, 1, 2, 3, 4)$ with the fixed gain $\rho_{fixed} = 0.435$.

and $x_{i2}(t)$ for different α values. As shown in Figures 7–8, the time to achieve consensus increases as α increases.

5. Conclusions

In this paper, a new FOMASs with parameter uncertainties and T-S membership functions has been developed on a directed communication topology graph. The distributed TSF impulsive controllers have been created to achieve the with/without leader exponential consensus. In addition, several sufficient criteria are also given in the forms of LMIs.

Future work will focus on the consensus problem for heterogeneous FOMASs with variable-order.

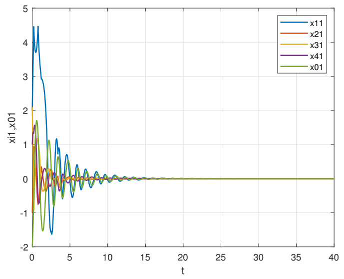

(a) $\alpha = 0.7$

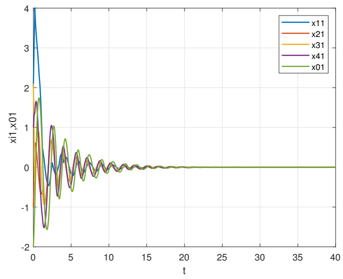

(b) $\alpha = 0.74$

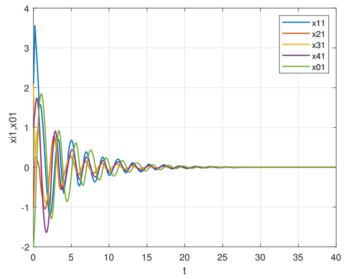

(c) $\alpha = 0.79$

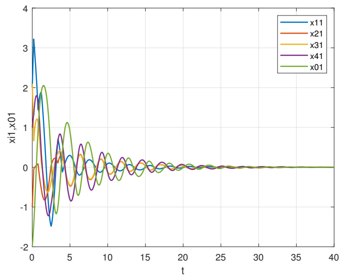

(d) $\alpha = 0.84$

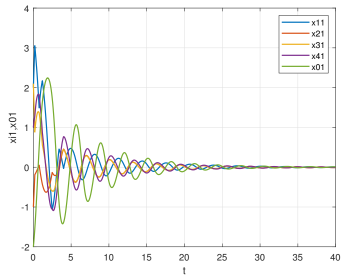

(e) $\alpha = 0.87$

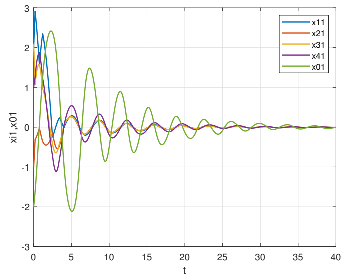

(f) $\alpha = 0.90$

Figure 7. The evolution of system state $x_{i1}(t)$ and $x_{01}(t)$ for different α values.

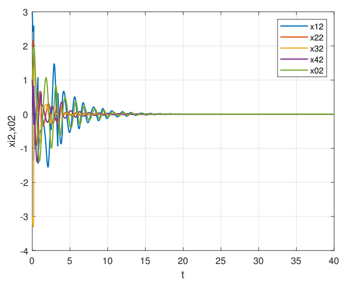

(a) $\alpha = 0.7$

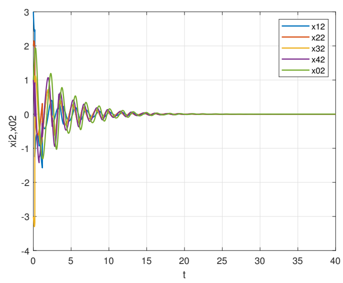

(b) $\alpha = 0.74$

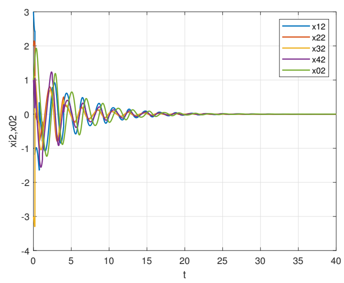

(c) $\alpha = 0.79$

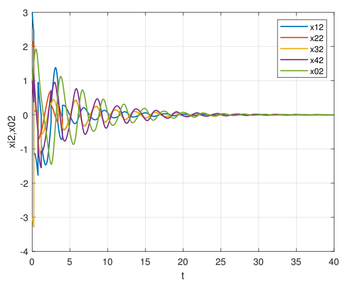

(d) $\alpha = 0.84$

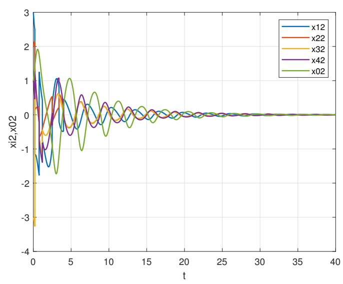

(e) $\alpha = 0.87$

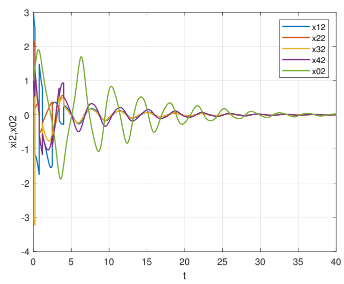

(f) $\alpha = 0.90$

Figure 8. The evolution of system state $x_{i2}(t)$ and $x_{02}(t)$ for different α values.

Use of AI tools declaration

The authors declare they have not used Artificial Intelligence (AI) tools in the creation of this article.

Acknowledgments

This work was supported by the Natural Science Foundation of China (No.12171416).

Conflict of interest

The authors declare there are no conflicts of interest.

References

1. J. A. Guerrero, G. Romero, D. Olivares, L. M. Romero-Cruz, Forced multi-agent bipartite consensus control: Application to quadrotor formation flying, *IEEE Access*, **12** (2024), 163654–163670. https://doi.org/10.1109/ACCESS.2024.3489422
2. S. N. Campos-Martínez, O. Hernández-González, M. E. Guerrero-Sánchez, G. Valencia-Palomo, B. Targui, F. R. López-Estrada, Consensus tracking control of multiple unmanned aerial vehicles subject to distinct unknown delays, *Machines*, **12** (2024), 337. https://doi.org/10.3390/machines12050337
3. C. Yu, X. Wang, X. Xu, M. Zhang, H. Ge, J. Ren, et al., Distributed multiagent coordinated learning for autonomous driving in highways based on dynamic coordination graphs, *IEEE Trans. Intell. Transp. Syst.*, **21** (2019), 735–748. https://doi.org/10.1109/TITS.2019.2893683
4. Y. Zhao, G. Guo, Distributed tracking control of mobile sensor networks with intermittent communications, *J. Franklin Inst.*, **354** (2017), 3634–3647. https://doi.org/10.1016/j.jfranklin.2017.03.003
5. F. R. López-Estrada, H. Darias, V. Puig, G. Valencia-Palomo, J. Domínguez-Zenteno, M. E. Guerrero-Sánchez, Cooperative convex control of multiagent systems applied to differential drive robots, *Int. J. Appl. Math. Comput. Sci.*, **34** (2024), 199–210. https://doi.org/10.61822/amcs-2024-0014
6. X. Hou, H. Wu, J. Cao, Practical finite-time synchronization for Lur'e systems with performance constraint and actuator faults: A memory-based quantized dynamic event-triggered control strategy, *Appl. Math. Comput.*, **487** (2025), 129108. https://doi.org/10.1016/j.amc.2024.129108
7. H. Wu, X. Zhao, L. Wang, J. Cao, Observer-based fixed-time topology identification and synchronization for complex networks via quantized pinning control strategy, *Appl. Math. Comput.*, **507** (2025), 129568. https://doi.org/10.1016/j.amc.2025.129568
8. X. Zhao, H. Wu, J. Cao, L. Wang, Prescribed-time synchronization for complex dynamic networks of piecewise smooth systems: A hybrid event-triggering control approach, *Qual. Theory Dyn. Syst.*, **24** (2025), 11. https://doi.org/10.1007/s12346-024-01166-x

9. J. A. V. Trejo, J. C. Ponsart, M. Adam-Medina, G. Valencia-Palomo, Fault-tolerant observer-based leader-following consensus control for LPV multi-agent systems using virtual actuators, *Int. J. Syst. Sci.*, **56** (2025), 1816–1833. https://doi.org/10.1080/00207721.2024.2434895

10. L. Cai, B. Zhang, M. Xing, H. Mo, X. Zhou, Consensus control of multi-agent systems by intermittent brownian noise stabilization scheme, *IEEE Access*, **12** (2024), 8526–8535. https://doi.org/10.1109/ACCESS.2024.3352441

11. T. Chen, F. Wang, C. Xia, Z. Chen, Leader-following consensus of second-order multi-agent systems with intermittent communication via persistent-hold control, *Neurocomputing*, **471** (2022), 183–193. https://doi.org/10.1016/j.neucom.2021.10.111

12. Y. Xin, H. Lyu, H. Tuo, Z. Cheng, Event-based consensus for third-order nonlinear multi-agent systems, *Chaos Solitons Fractals*, **169** (2023), 113269. https://doi.org/10.1016/j.chaos.2023.113269

13. J. Dai, C. Yang, X. Yan, J. Wang, K. Zhu, C. Yang, Leaderless consensus control of nonlinear PIDE-type multi-agent systems with time delays, *IEEE Access*, **10** (2022), 21211–21218. https://doi.org/10.1109/ACCESS.2022.3153078

14. W. Zhu, B. Chen, J. Yang, Consensus of fractional-order multi-agent systems with input time delay, *Fract. Calc. Appl. Anal.*, **20** (2017), 52–70. https://doi.org/10.1515/fca-2017-0003

15. Z. Yu, H. Jiang, C. Hu, J. Yu, Necessary and sufficient conditions for consensus of fractional-order multiagent systems via sampled-data control, *IEEE Trans. Cybern.*, **47** (2017), 1892–1901. https://doi.org/10.1109/TCYB.2017.2681718

16. P. Xiao, Z. Gu, Adaptive event-triggered consensus of fractional-order nonlinear multi-agent systems, *IEEE Access*, **10** (2021), 213–220. https://doi.org/10.1109/ACCESS.2021.3136892

17. P. Gong, W. Lan, Adaptive robust tracking control for uncertain nonlinear fractional-order multi-agent systems with directed topologies, *Automatica*, **92** (2018), 92–99. https://doi.org/10.1016/j.automatica.2018.02.010

18. X. Wang, H. Wu, J. Cao, Global leader-following consensus in finite time for fractional-order multi-agent systems with discontinuous inherent dynamics subject to nonlinear growth, *Nonlinear Anal. Hybrid Syst.*, **37** (2020), 100888. https://doi.org/10.1016/j.nahs.2020.100888

19. G. Ren, Y. Yu, Consensus of fractional multi-agent systems using distributed adaptive protocols, *Asian J. Control*, **19** (2017), 2076–2084. https://doi.org/10.1002/asjc.1589

20. X. Su, F. Xia, J. Liu, L. Wu, Event-triggered fuzzy control of nonlinear systems with its application to inverted pendulum systems, *Automatica*, **94** (2018), 236–248. https://doi.org/10.1016/j.automatica.2018.04.025

21. D. Saifia, M. Chadli, H. R. Karimi, S. Labiod, Fuzzy control for electric power steering system with assist motor current input constraints, *J. Franklin Inst.*, **352** (2015), 562–576. https://doi.org/10.1016/j.jfranklin.2014.05.007

22. D. J. Singh, N. K. Verma, A. K. Ghosh, A. Malagaudanavar, An application of interval type-2 fuzzy model based control system for generic aircraft, *Appl. Soft Comput.*, **121** (2022), 108721. https://doi.org/10.1016/j.asoc.2022.108721

23. J. Li, Z. Jin, Y. Zhang, Optimal output agreement for TS fuzzy multi-agent systems: an adaptive distributed approach, *Int. J. Fuzzy Syst.*, **25** (2023), 2453–2463. https://doi.org/10.1007/s40815-023-01493-2

24. Y. Cheng, T. Hu, Y. Li, X. Zhang, S. Zhong, Delay-dependent consensus criteria for fractional-order Takagi-Sugeno fuzzy multi-agent systems with time delay, *Inf. Sci.*, **560** (2021), 456–475. https://doi.org/10.1016/j.ins.2021.01.074

25. T. Ma, Z. Zhang, B. Cui, Impulsive consensus of nonlinear fuzzy multi-agent systems under DoS attack, *Nonlinear Anal. Hybrid Syst.*, **44** (2022), 101155. https://doi.org/10.1016/j.nahs.2022.101155

26. G. He, J. Zhao, Leader-following output consensus of T-S fuzzy switched multi-agent systems under bumpless transfer control and event-triggered communication, *Neurocomputing*, **506** (2022), 252–264. https://doi.org/10.1016/j.neucom.2022.07.064

27. T. Hu, Z. He, X. Zhang, S. Zhong, Event-triggered consensus strategy for uncertain topological fractional-order multiagent systems based on Takagi-Sugeno fuzzy models, *Inf. Sci.*, **551** (2021), 304–323. https://doi.org/10.1016/j.ins.2020.11.005

28. Z. Hu, X. Mu, J. Mu, Finite-time impulsive control for stochastic T-S fuzzy systems: A waiting-time-based event-triggered method, *Fuzzy Sets Syst.*, **464** (2023), 108428. https://doi.org/10.1016/j.fss.2022.10.020

29. G. Narayanan, M. S. Ali, H. Alsulami, G. Stamov, I. Stamova, B. Ahmad, Impulsive security control for fractional-order delayed multi-agent systems with uncertain parameters and switching topology under DoS attack, *Inf. Sci.*, **618** (2022), 169–190. https://doi.org/10.1016/j.ins.2022.10.123

30. Z. Gao, H. Zhang, Y. Wang, K. Zhang, Leader-following consensus conditions for fractional-order descriptor uncertain multi-agent systems with $0 < \alpha < 2$ via output feedback control, *J. Franklin Inst.*, **357** (2020), 2263–2281. https://doi.org/10.1016/j.jfranklin.2019.11.047

31. F. Wang, Y. Yang, Leader-following exponential consensus of fractional order nonlinear multi-agents system with hybrid time-varying delay: A heterogeneous impulsive method, *Physica A*, **482** (2017), 158–172. https://doi.org/10.1016/j.physa.2017.04.049

32. S. Dong, K. Shi, X. Xie, M. Yu, H. Yan, X. Cai, Fuzzy-based synchronization control for coupled neural networks under cyber attacks via intelligent impulsive algorithm, *IEEE Trans. Autom. Sci. Eng.*, **22** (2025), 10574–10585. https://doi.org/10.1109/TASE.2025.3525658

33. S. Yang, W. Zhang, D. Ruan, T. Yang, Y. Li, Fast fixed-time impulsive bipartite synchronization of T-S fuzzy complex networks with signed graphs, *Nonlinear Anal. Hybrid Syst.*, **48** (2023), 101325. https://doi.org/10.1016/j.nahs.2022.101325

34. M. Hu, J. H. Park, Y. Wang, Stabilization of positive systems with time delay via the Takagi-Sugeno fuzzy impulsive control, *IEEE Trans. Cybern.*, **52** (2020), 4275–4285. https://doi.org/10.1109/TCYB.2020.3025639

35. B. Hu, Z. Guan, X. Yu, Q. Luo, Multisynchronization of interconnected memristor-based impulsive neural networks with fuzzy hybrid control, *IEEE Trans. Fuzzy Syst.*, **26** (2018), 3069–3084. https://doi.org/10.1109/TFUZZ.2018.2797952

36. H. Nie, Y. Zhang, Finite-time cluster synchronization of multi-weighted fractional-order coupled neural networks with and without impulsive effects, *Neural Networks*, **180** (2024), 106646. https://doi.org/10.1016/j.neunet.2024.106646

37. S. Yang, C. Hu, J. Yu, H. Jiang, Exponential stability of fractional-order impulsive control systems with applications in synchronization, *IEEE Trans. Cybern.*, **50** (2019), 3157–3168. https://doi.org/10.1109/TCYB.2019.2906497

38. M. Yao, G. Wei, Dynamic event-triggered control of continuous-time systems with random impulses, *IEEE/CAA J. Autom. Sin.*, **10** (2023), 2292–2299. https://doi.org/10.1109/JAS.2023.123534

39. I. Stamova, J. Henderson, Practical stability analysis of fractional-order impulsive control systems, *ISA Trans.*, **64** (2016), 77–85. https://doi.org/10.1016/j.isatra.2016.05.012

AIMS Press

© 2026 the Author(s), licensee AIMS Press. This is an open access article distributed under the terms of the Creative Commons Attribution License (https://creativecommons.org/licenses/by/4.0)